

1 Cell-specific Bioorthogonal Tagging of Glycoproteins

2 Anna Cioce^{a,b}, Beatriz Calle^{a,b}, Tatiana Rizou^{c,§}, Sarah C. Lowery^{d,§}, Victoria Bridgeman^{e,§}, Keira E.
3 Mahoney^{d,§}, Andrea Marchesi^{a,b}, Ganka Bineva-Todd^b, Helen Flynn^e, Zhen Li^{a,b}, Omur Y. Tastan^b,
4 Chloe Roustan^f, Pablo Soro-Barrio^g, Thomas M. Wood^{h,k}, Tessa Keenanⁱ, Peter Both^j, Kun Huang^{j,l},
5 Fabio Parmeggiani^{j,m}, Ambrosius P. Snijders^e, Mark Skehel^e, Svend Kjaer^f, Martin A. Fascioneⁱ,
6 Carolyn R. Bertozzi^h, Sabine Flitsch^j, Stacy A. Malaker^d, Ilaria Malanchi^c, Benjamin Schumann^{a,b,*}

7 ^aDepartment of Chemistry, Imperial College London, 80 Wood Lane, W12 0BZ, London, United
8 Kingdom.

9 ^bChemical Glycobiology Laboratory, The Francis Crick Institute, 1 Midland Rd, NW1 1AT London,
10 United Kingdom.

11 ^cTumour-Host Interaction Laboratory, The Francis Crick Institute, 1 Midland Rd, NW1 1AT London,
12 United Kingdom.

13 ^dDepartment of Chemistry, Yale University, 275 Prospect Street, New Haven, CT 06511, United States.

14 ^eProteomics Science Technology Platform, The Francis Crick Institute, NW1 1AT London, United
15 Kingdom.

16 ^fStructural Biology Science Technology Platform, The Francis Crick Institute, NW1 1AT London,
17 United Kingdom.

18 ^gBioinformatics & Biostatistics Science Technology Platform, The Francis Crick Institute, NW1 1AT
19 London, United Kingdom.

20 ^hDepartment of Chemistry, Stanford University, Stanford, CA 94305, USA.

21 ⁱDepartment of Chemistry, University of York, YO10 5DD York, United Kingdom.

22 ^jManchester School of Chemistry & Institute of Biotechnology, The University of Manchester, M1
23 7DN Manchester, United Kingdom.

24 ^{k,l}current address: Massachusetts Institute of Technology, Cambridge, USA

25 ^lcurrent address: Department of Chemistry and Biochemistry, University of Maryland, Baltimore, MD
26 21250, USA.

27 ^mcurrent address: Department of Chemistry, Materials and Chemical Engineering “G. Natta”,
28 Politecnico di Milano, 20131 Milano, Italy

29 [§]These authors contributed equally.

30 ^{*}Correspondence should be addressed to: b.schumann@imperial.ac.uk.

31

32

33

34 ABSTRACT

35 Altered glycosylation is an undisputed corollary of cancer development. Understanding these alterations is
36 paramount but hampered by limitations underlying cellular model systems. For instance, the intricate
37 interactions between tumour and host cannot be adequately recapitulated in monoculture of tumour-derived cell
38 lines. More complex co-culture models usually rely on sorting procedures for proteome analyses and rarely
39 capture the details of protein glycosylation. Here, we report a strategy termed Bio-Orthogonal Cell line-specific
40 Tagging of Glycoproteins (BOCTAG). Cells are equipped by transfection with an artificial biosynthetic
41 pathway that transforms bioorthogonally tagged sugars into the corresponding nucleotide-sugars. Only
42 transfected cells incorporate bioorthogonal tags into glycoproteins in the presence of non-transfected cells. We
43 employ BOCTAG as an imaging technique and to annotate cell-specific glycosylation sites in mass
44 spectrometry-glycoproteomics. We demonstrate application in co-culture and mouse models, allowing for
45 profiling of the glycoproteome as an important modulator of cellular function.

46 INTRODUCTION

47 Cancer is a multifactorial disease consisting of an interplay between different host and tumour cells. Emulating
48 the complexity of a tumour using cell monoculture is thus incomplete by design, requiring more elaborated co-
49 culture systems or *in vivo* models.¹⁻³ Recent years have seen a stark increase in methods to probe the
50 transcriptomes of tumour and host cell populations, respectively, providing some insight into their state within a
51 multicellular conglomerate.⁴ However, the relationship between transcriptome and proteome is still elusive.⁵ In
52 addition, posttranslational modifications (PTMs) heavily impact the plasticity of the proteome. Glycosylation is
53 the most complex and most abundant PTM, but challenging to probe due to the non-templated nature of glycan
54 biosynthesis.⁶ Glycans are generated by the combinatorial interplay of >250 glycosyltransferases (GTs) and
55 glycosidases, mostly in the secretory pathway.⁷ Certain glycoproteins aberrantly expressed in cancer, such as
56 mucins, are approved as diagnostic markers, but their discovery is a particular challenge.^{8,9} This is especially
57 true when *in vivo* or *in vitro* model systems comprise cell populations from the same organism that do not allow
58 distinction of proteomes by amino acid sequence.^{10,11} Methods to study the glycoproteome of a cell type in co-
59 culture or *in vivo* are therefore an unmet need.

60 Metabolic oligosaccharide engineering (MOE) produces chemical reporters of glycan subtypes.¹² MOE reagents
61 are membrane permeable monosaccharide precursors modified with chemical tags amenable to bioorthogonal
62 chemistry.¹³ Following incorporation into the glycoproteome, chemical tags are reacted with traceable
63 enrichment handles or fluorophores, for instance by Cu(I)-catalysed azide-alkyne cycloaddition (CuAAC).^{14,15}
64 Many MOE reagents are based on analogues of sugars such as *N*-acetylgalactosamine (GalNAc) that are
65 straightforward to chemically tag by replacing the acetamide with bioorthogonal *N*-acylamides (Fig. 1a).
66 Unmodified GalNAc is normally activated by the biosynthetic GalNAc salvage pathway to the nucleotide-sugar
67 UDP-GalNAc that can follow two major distinct metabolic fates (Fig. 1a).^{14,16-18} First, the 20 members of the
68 GalNAc transferase family (GalNAc-T1...T20) use UDP-GalNAc to form the linkage GalNAc α -Ser/Thr and
69 thereby prime cancer-relevant O-GalNAc glycans.^{14,19,20} Second, epimerisation at the GalNAc C4 position by
70 the UDP-galactose-4-epimerase (GALE) yields UDP-*N*-acetylglucosamine (UDP-GlcNAc) that can be
71 incorporated into different glycan subtypes, for instance Asn-linked N-glycans.^{17,18,21} Certain chemical

72 modifications at the *N*-acyl moiety can render GalNAc analogues recalcitrant to these metabolic processes. For
73 instance, analogues of UDP-GalNAc with long alkyne-containing *N*-acyl substituents are not biosynthesised by
74 the GalNAc salvage pathway and not used as substrates by wild type (WT)-GalNAc-Ts.^{18,22–24} While being a
75 substantial impediment to generating MOE reporters, we realised that overcoming these metabolic roadblocks
76 might enable programmable bioorthogonal glycoprotein tagging. Such a strategy would allow for studying the
77 glycoproteome in a cell-specific fashion, which is currently elusive despite the rapid advances in the
78 development of new MOE reagents.

79 Here, we develop a technique called Bio-Orthogonal Cell-specific Tagging of Glycoproteins (BOCTAG). The
80 strategy uses an artificial biosynthetic pathway to generate alkyne-tagged UDP-GalNAc and UDP-GlcNAc
81 analogues from a readily available GalNAc precursor that is not accepted by the GalNAc salvage pathway. We
82 find that a single methylene group between 5-carbon (GalNAk) and 6-carbon (GalN6yne) *N*-acyl substituents
83 drastically reduces uptake by the native GalNAc salvage pathway and thereby reduces the background of
84 bioorthogonal labelling in non-transfected cells. Only cells carrying the artificial pathway biosynthesise the
85 corresponding UDP-sugars (UDP-GalN6yne and UDP-GlcN6yne) that are then used by GTs to chemically tag
86 the glycoproteome. We further expand the strategy with mutant GalNAc-Ts that are engineered to accept UDP-
87 GalN6yne as a substrate. The combined use of an artificial biosynthetic pathway and engineered GalNAc-Ts
88 enables GalN6yne-mediated fluorescent labelling of the cellular glycoproteome that is two orders of magnitude
89 higher than in cells carrying neither component. We demonstrate that BOCTAG allows for programmable
90 glycoprotein tagging in co-culture and mouse models. Moreover, the nature of the artificial biosynthetic
91 pathway allowed for the use of readily available Ac₄GalN6yne as a precursor with enhanced stability over
92 previously used caged GalN6yne-1-phosphates as an essential pre-requisite for *in vivo* applications. We show
93 that the chemical modification enters a range of glycan subtypes, supporting the use of BOCTAG to tag a large
94 number of glycoproteins in complex biological systems.

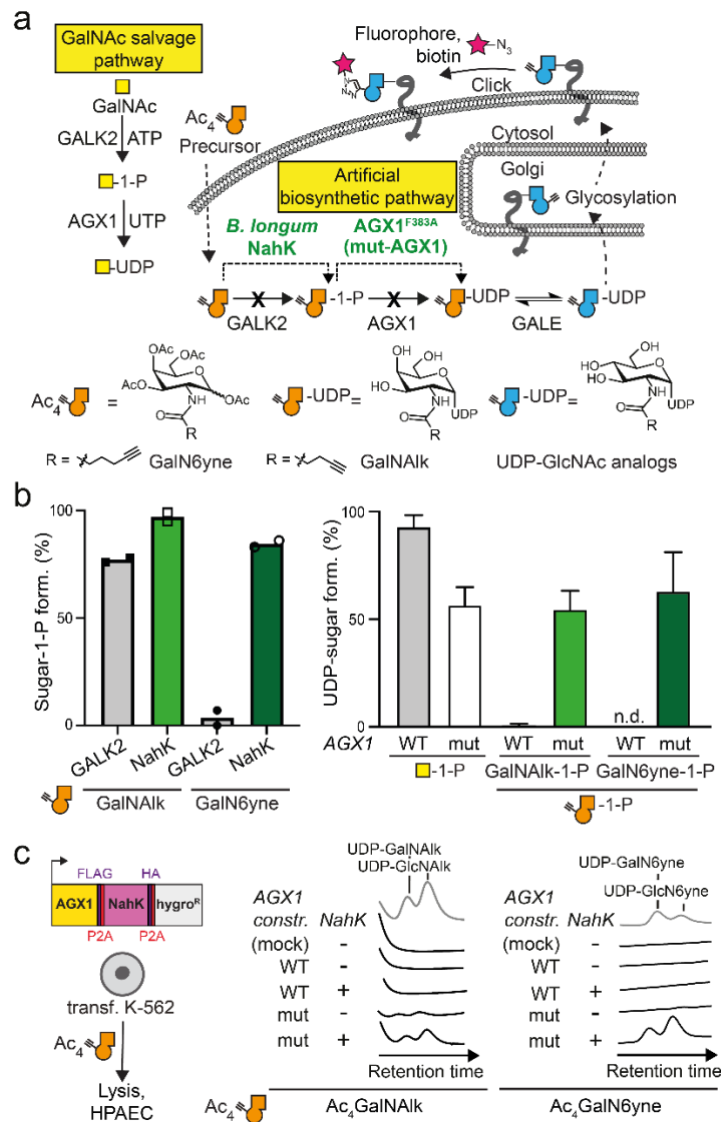
95 RESULTS

96 **Developing an artificial biosynthetic pathway for chemically tagged UDP-sugars.**

97 The human GalNAc salvage pathway consists of the kinase GALK2 and the pyrophosphorylases AGX1/2 to
98 convert GalNAc first into GalNAc-1-phosphate and subsequently into UDP-GalNAc, respectively (Fig. 1a).
99 Since neither analogues of GalNAc nor GalNAc-1-phosphate can be utilized by any other metabolic enzyme,
100 the GalNAc salvage pathway was deemed suitable for monitoring conversions of each step while supplying
101 readily accessible synthetic, bioorthogonal precursors. GALK2 and AGX1/2 are impervious to large chemical
102 modifications at the *N*-acyl moiety of GalNAc (Fig. 1a), corroborated by crystal structures of these enzymes
103 (Fig. S1).^{18,25–27} An artificial biosynthetic pathway was thus designed to convert chemically tagged GalNAc
104 analogues first to the corresponding sugar-1-phosphates and subsequently to the UDP-sugars. We chose both a
105 6-carbon hex-5-ynoate chain (GalN6yne) and a 5-carbon pent-4-ynoate chain (GalNAk) as GalNAc
106 modifications due to their availability and previous use by us and others.^{18,27,28} In *in vitro* enzymatic assays
107 detected by liquid chromatography-mass spectrometry (LC-MS), recombinant GALK2 accepted GalNAk as a
108 substrate, but only marginally accepted GalN6yne (Fig. 1b). In contrast, promiscuous bacterial *N*-
109 acetylhexosaminylnyl kinases (NahK) from various source organisms converted GalN6yne to GalN6yne-1-

110 phosphate almost quantitatively (Fig. 1b, fig. S2a).²⁹ Similarly, the pyrophosphorylase AGX1 showed little to
111 no turnover of both GalNA1k-1-phosphate and GalN6yne-1-phosphate to the corresponding UDP-sugars (Fig.
112 1b). We and others have mutated AGX1 at residue Phe383 to smaller amino acids to accommodate chemical *N*-
113 acyl modifications.^{27,30} AGX1^{F383A}, herein called mut-AGX1, converted both synthetic GalNA1k-1-phosphate
114 and GalN6yne-1-phosphate to UDP-GalNA1k and UDP-GalN6yne, respectively (Fig. 1b).

115 We next assessed UDP-sugar biosynthesis in the living cell. Stable bicistronic expression of a codon-optimized
116 version of *Bifidobacterium longum* NahK as well as mut-AGX1 in K-562 cells biosynthesized UDP-GalNA1k
117 and UDP-GalN6yne from membrane-permeable per-acetylated precursors Ac₄GalNA1k and Ac₄GalN6yne,
118 respectively (Fig. 1c). Expression of either enzyme alone or WT-AGX1 led to inefficient biosynthesis compared
119 to levels of native UDP-sugars (Fig. S3). We confirmed these results by feeding cells a caged precursor of
120 GalN6yne-1-phosphate that was uncaged in the living cell and converted to UDP-GalN6yne only in the
121 presence of mut-AGX1 (Fig. S3). Alkyne-tagged UDP-GalNAc analogues were converted to the corresponding
122 UDP-GlcNAc analogues (UDP-GlcNA1k or UDP-GlcN6yne, respectively) in cells by the epimerase GALE,
123 which was corroborated in an *in vitro* epimerisation assay (Fig. 1a,c fig. S2b, fig. S3). Thus, installing an
124 artificial biosynthetic pathway led to programmable biosynthesis of alkyne-tagged analogues of UDP-GalNAc
125 and UDP-GlcNAc.



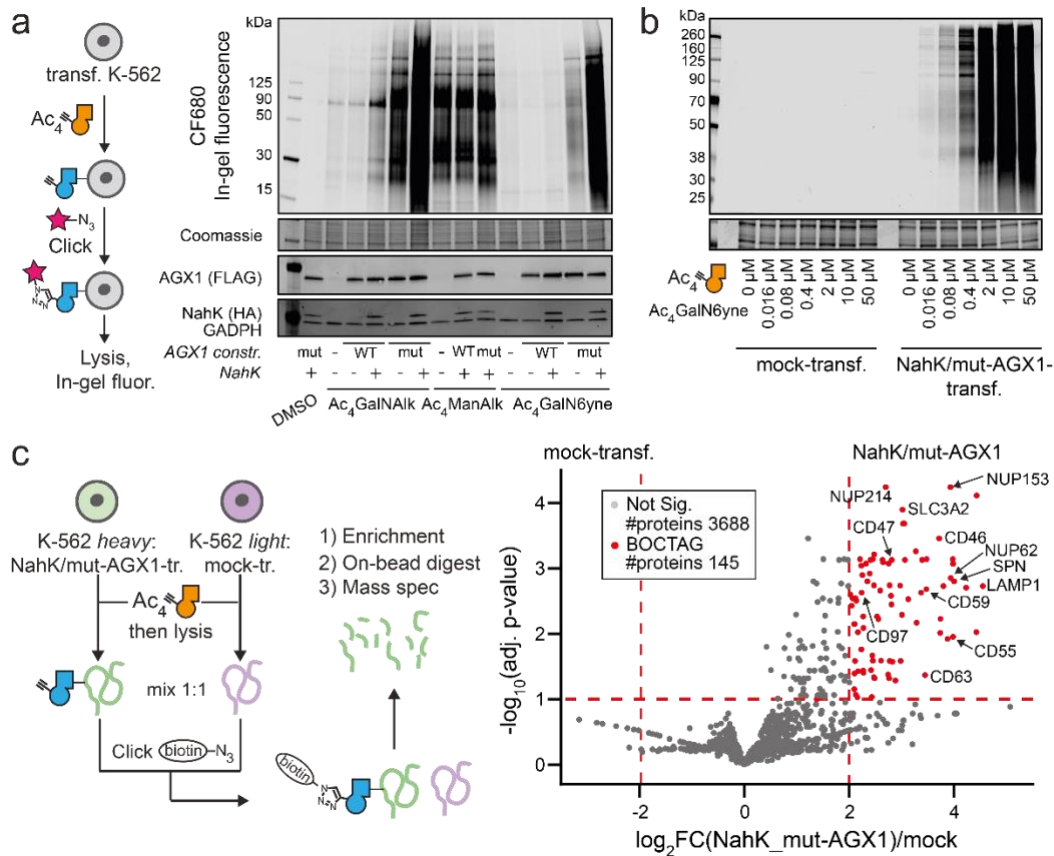
126

127 **Fig. 1: Development of an artificial biosynthetic pathway for chemically tagged UDP-GalNAc/GlcNAc**
 128 **analogues. a**, strategy of metabolic oligosaccharide engineering. A chemically modified GalNAc analogue that
 129 is not accepted by the GalNAc salvage pathway should be processed by an artificial biosynthetic pathway. *B.*
 130 *longum* NahK and mut-AGX1 biosynthesize UDP-GalNAc analogues and, by epimerisation, UDP-GlcNAc
 131 analogues. Incorporation into glycoconjugates can be traced by CuAAC. **b**, *in vitro* evaluation of GalNAc-1-
 132 phosphate analogue synthesis by human GALK2 or *B. longum* NahK (left) and UDP-GalNAc analogue
 133 synthesis by WT- or mut-AGX1 (right). Data were recorded in LC-MS assays and processed by integrated ion
 134 counts. Data are from two independent experiments and depicted as individual data points and means (left) or
 135 from three independent experiments and depicted as means + standard deviation (SD, right). **c**, biosynthesis of
 136 UDP-GalNAc/GlcNAc analogues in cells stably expressing both NahK and mut-AGX1 or either component, as
 137 assessed by high performance anion exchange chromatography (HPAEC). A hygromycin resistance gene allows
 138 for stable transfection. Data are representative of one out of two independent experiments collected on two
 139 different days. mock: pSBbi-GH empty plasmid.

140

141 We next assessed chemical tagging of the cell surface glycoproteome in living cells. K-562 cells stably
142 expressing combinations of NahK and AGX1 were fed with DMSO, Ac₄GalNAIk or Ac₄GalN6yne and reacted
143 with the clickable fluorophore CF680-picolyl azide by CuAAC. The MOE reagent Ac₄ManAlk that enters the
144 pool of the sugar sialic acid was included as a positive control. Alkyne tags were visualized by in-gel
145 fluorescence after cell lysis (Fig. 2a). While Ac₄GalNAIk feeding led to high-intensity fluorescent signal when
146 NahK and mut-AGX1 were expressed, substantial signal was observed in cells expressing WT-AGX1 when
147 NahK was present (Fig. 2a). Fluorescent signal after Ac₄GalNAIk feeding was also observed in cells transfected
148 with an empty plasmid or only overexpressing WT-AGX1, confirming the permissiveness of the GalNAc
149 salvage pathway for GalNAIk (Fig. 1b).¹⁸ In contrast, Ac₄GalN6yne incorporation was critically dependent on
150 the expression of mut-AGX1, while the presence of NahK led to a further sixfold increase in fluorescence
151 intensity (Fig. 2a). Ac₄ManAlk gave fluorescent signal regardless of the enzyme combination expressed. Dose
152 response experiments showed that Ac₄GalN6yne-mediated fluorescence intensity increased over two orders of
153 magnitude with the concentration of the probe between 16 nM and 50 μM only when NahK and mut-AGX1
154 were present (Fig. 2b). Transfection and feeding with chemically modified sugars can in theory alter the cellular
155 transcriptome, leading to artifacts in protein expression and metabolic labelling. We performed transcriptomic
156 analyses in cells transfected with either NahK/mut-AGX1 or empty plasmid, and fed with either DMSO vehicle,
157 Ac₄GalN6yne or Ac₄GalNAc. By performing correlation plot and principal component analysis (PCA)(Fig. S4),
158 we observed that the day of sample collection has a greater effect on transcript levels than either transgene
159 expression or compound treatment (Fig. S4b). These data suggest that neither artificial biosynthetic pathway nor
160 compound feeding has substantial effects on the transcriptome. Due to the robustness of metabolic
161 incorporation, we used Ac₄GalN6yne as an MOE reagent for all subsequent applications of BOCTAG.

162



163

164 **Fig. 2: An artificial biosynthetic pathway enables programmable chemical tagging of the glycoproteome.**

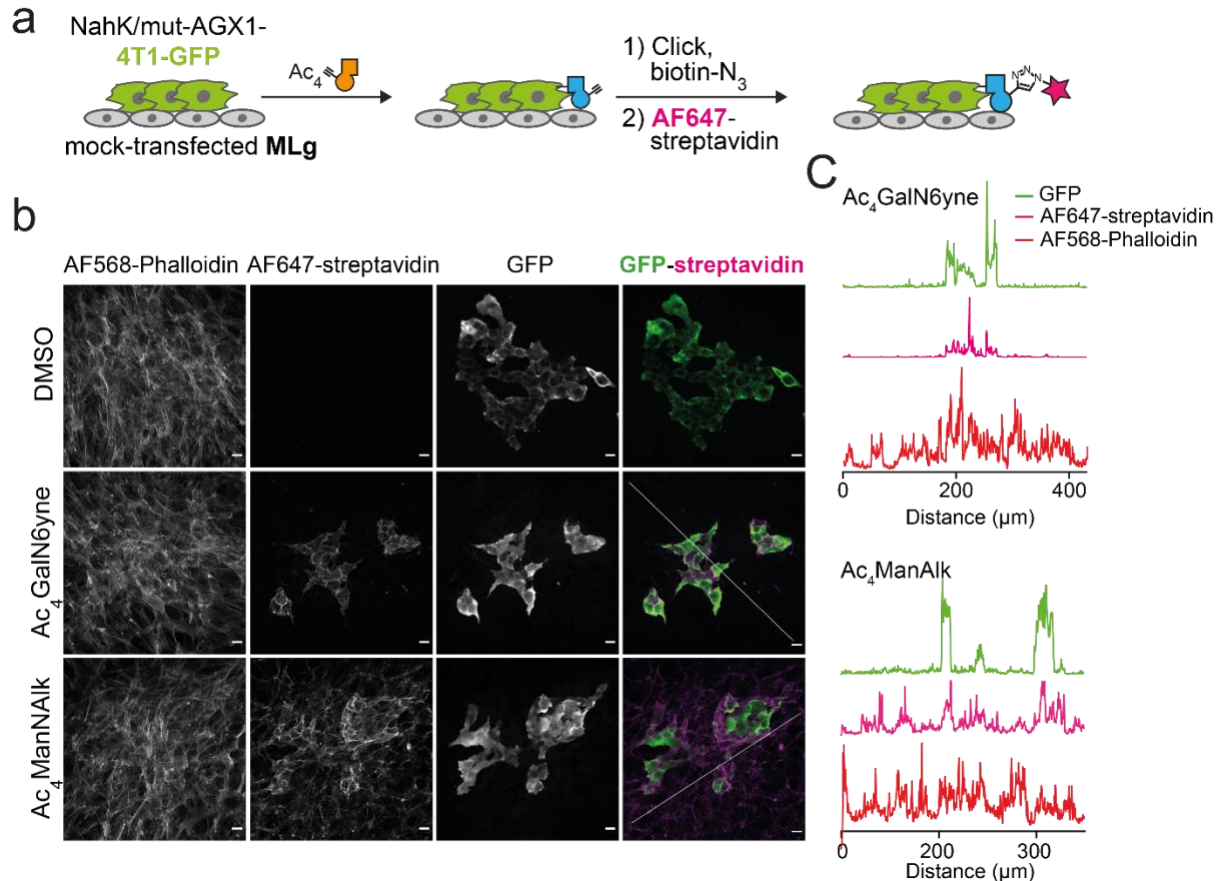
165 **a**, evaluation of cell surface glycoproteome tagging after treating K-562 cells stably expressing NahK/AGX1
 166 combinations with 50 μM Ac₄GalNAk, 50 μM Ac₄GalN6yne or 10 μM Ac₄ManNAk. Glycoproteins were
 167 visualised by in-gel fluorescence after treating cells with CF680-picolyl azide under CuAAC conditions and
 168 subsequent cell lysis. **b**, dose-response experiment of cell surface glycoproteome tagging, with samples
 169 processed as in **a**. Data in **a** and **b** are representative of one out of two independent experiments. **c**, quantitative
 170 measurement of glycoprotein tagging by SILAC. Data were analysed from three independent experiments,
 171 collected on three different days, with forward (heavy mock, light NahK/mut-AGX1) and reverse (light mock,
 172 heavy NahK/mut-AGX1) analyses incorporated as a total of six replicates. Data are visualised as volcano plot,
 173 choosing 4-fold enrichment and a p-value of 0.1 as cut-offs, with example glycoproteins annotated. Significance
 174 levels were indicated. mock: pSBbi-GH empty plasmid.

175

176 **An artificial biosynthetic pathway allows for programmable enrichment of the glycoproteome.**

177 We used Stable Isotope Labelling by Amino Acids in Cell Culture (SILAC)-based proteome analysis to confirm
 178 and quantify chemical glycoproteome tagging. K-562 cells transfected with NahK/mut-AGX1 or an empty
 179 plasmid (mock-transfected). Both were individually grown in heavy or light media in the presence of either
 180 Ac₄GalN6yne or DMSO. Lysates of these cells were mixed as different combinations to contain equal amounts
 181 of heavy and light protein, and clickable biotin-picolyl azide was installed on tagged glycoproteins by CuAAC.
 182 Enrichment on neutravidin beads followed by on-bead digest allowed analysis by quantitative mass

183 spectrometry (MS). In three independent experiments in which both combinations of heavy and light SILAC
184 labelling each were used (Fig. 2c), we found peptides from 145 proteins to be significantly enriched in
185 NahK/mut-AGX1-transfected cells (Supplementary Table1). More than 99% (143/145) of these proteins have
186 been previously annotated³¹⁻³³ as either N- or O-glycosylated, including the nucleoporins Nup62 and Nup153
187 and the cell surface proteins CD47 and NOTCH1, confirming the stringency of the approach for tagging
188 glycoproteins.



189
190 **Fig. 3: Bioorthogonal cell-specific glycoprotein tagging in co-culture.** **a**, schematic of the 4T1-MLg co-
191 culture experiment. Green fluorescent protein (GFP)-expressing 4T1 cells transfected with NahK/mut-AGX1
192 should be selectively positive for AF647-labelling in BOCTAG. **b**, fluorescence microscopy, using co-cultures
193 fed with 50 μM Ac₄GalN6yne or 50 μM Ac₄ManNAIk as well as Alexafluor568-phalloidin as a counterstain. **c**,
194 intensity profile of fluorescent signal between GFP and AF647 in Ac₄GalN6yne- (top) or Ac₄ManNAIk-fed
195 (bottom) co-cultures. Scale bar, 20 μm. The intensity profile of GFP, AF647-Streptavidin and AF568-Phalloidin
196 signals was measured along a diagonal line drawn along the fluorescent image. Data are representative of one
197 out of two independent experiments.

198

199 Cell type-specific glycoproteome tagging in co-culture.

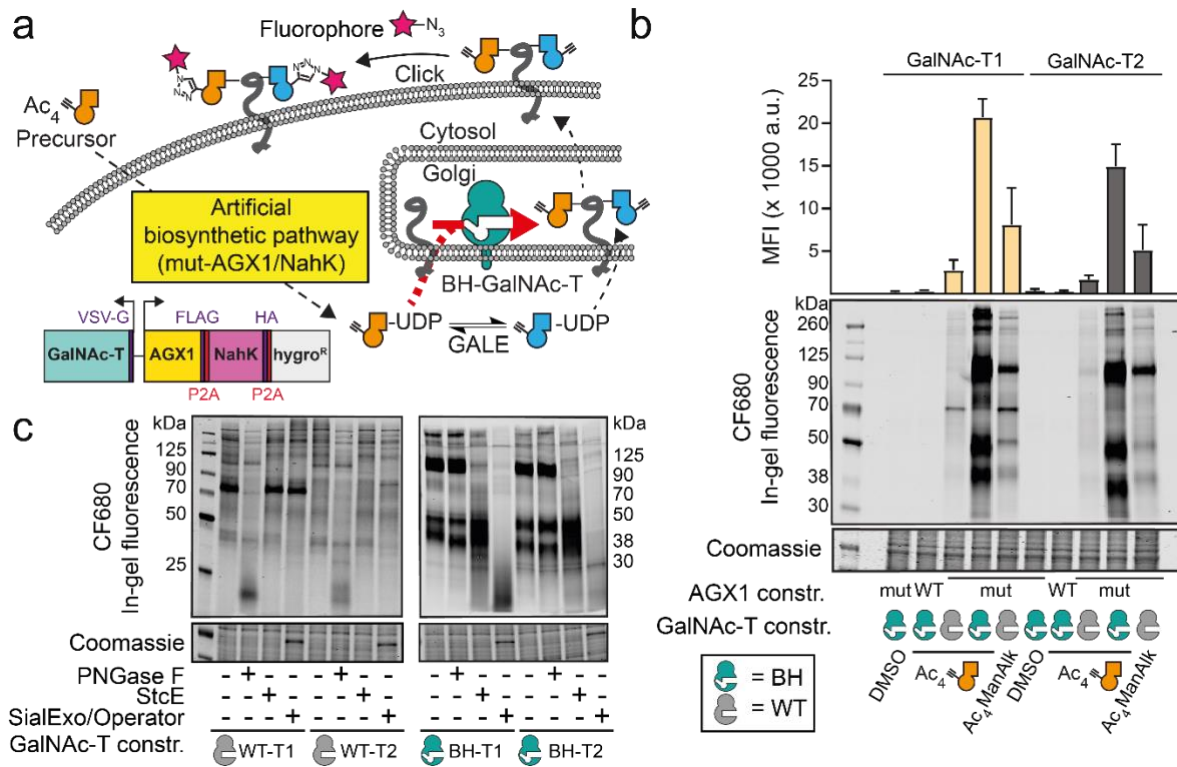
200 We next assessed the suitability of the artificial biosynthetic pathway NahK/mut-AGX1 as a BOCTAG cell
201 type-specific glycoproteome labelling technique by fluorescence microscopy. Colonies of NahK/mut-AGX1-

202 transfected and GFP-expressing 4T1 breast cancer cells were established on a monolayer of non-transfected
203 MLg fibroblast cells by co-culturing for 72 h before media supplementation with either Ac₄GalN₆yne,
204 Ac₄ManAlk or DMSO (Fig. 3a). Clickable biotin-picolyl azide was installed by CuAAC followed by
205 Streptavidin-AF647 staining to visualize chemical tagging, and cells were counter-stained with fluorescently
206 labelled phalloidin. Streptavidin-AF647 signal was strongly and reproducibly restricted to GFP-expressing cells
207 only when Ac₄GalN₆yne was fed and NahK/mut-AGX1 were expressed (Fig. 3b, C, fig. S5-S8), indicating a
208 localised BOCTAG signal. In contrast, the promiscuous MOE reagent Ac₄ManNAlk was non-specifically
209 incorporated throughout the entire co-culture (Fig. 3b, c, fig. S5-S8). When both GFP-4T1 and MLg cell lines
210 expressed NahK/mut-AGX1, both exhibited a strong Streptavidin-AF647 signal (Fig. S8b). Taken together,
211 BOCTAG enables cell-specific tagging of cell surface glycoproteins in co-culture.

212

213 **Assessing and manipulating the glycan types tagged by GalN₆yne.**

214 We next sought to assess and expand the glycan subtypes targeted by our MOE approach. We were prompted by
215 our recent findings that GalNAc analogues with bulky *N*-acyl chains such as GalN₆yne are not incorporated into
216 O-GalNAc glycans by WT-GalNAc-Ts (Fig. 4a).^{23,27,34} We have created GalNAc-T mutants termed BH-
217 GalNAc-Ts (for “bump-and-hole engineering”, the process used to design the mutants) that selectively use such
218 chemically tagged UDP-GalNAc analogues in glycosylation reactions.^{23,27,34} We stably co-expressed WT- or
219 BH-versions of GalNAc-T1 or T2 from plasmids also encoding NahK and mut-AGX1 in K-562 cells (Fig. 4a).
220 Expression of BH-GalNAc-Ts increased the intensity of in-gel fluorescence more than sevenfold over
221 expression of WT-GalNAc-Ts when cells were fed with Ac₄GalN₆yne (Fig. 4b). WT-AGX1 expressing cells
222 lacked UDP-GalN₆yne/UDP-GlcN₆yne biosynthesis and did not show any discernible fluorescent signal over
223 vehicle control DMSO (Fig. 1c). We assessed the subtypes of the chemically tagged glycans by digestion with
224 the hydrolytic enzymes PNGase F (reduces N-glycosylation), StcE (digests mucin-type glycoproteins) and
225 OpeRATOR (digests O-GalNAc glycoproteins in the presence of the sialidase SialEXO) prior to in-gel
226 fluorescence.³⁵ In cells expressing NahK, mut-AGX1 and WT-GalNAc-Ts, fluorescent labelling was slightly
227 sensitive to PNGase F treatment, indicating that the major target structures are N-glycoproteins in these cells
228 (Fig. 4c). Co-expression of BH-GalNAc-Ts led to additional highly intense fluorescent signal of a small number
229 of O-glycoproteins with sensitivity to both StcE and OpeRATOR/SialEXO (Fig. 4c). Thus, BH-GalNAc-Ts
230 broaden the target scope of chemical tagging to include O-GalNAc glycoproteins with high incorporation
231 efficiency. Concomitant with this finding, we performed quantitative MS-proteome analysis by SILAC of cell
232 lines expressing NahK/mut-AGX1/BH-GalNAc-T2 (BH-T2). In contrast to cells expressing only NahK/mut-
233 AGX1/WT-T2 (Fig. 2c), we observed an increase from 37% to 61% of O-GalNAc glycoproteins³¹⁻³³ in the
234 enriched protein fraction (Supplementary Table1).



235

236 **Fig. 4: Enhancement of programmable glycoprotein tagging by expression of BH-GalNAc-Ts.** **a**, strategy
 237 of expanding glycoprotein tagging to include O-GalNAc glycans. Expression of BH-GalNAc-Ts selectively
 238 engineered to accommodate bulky chemical tags enhances O-GalNAc tagging in cells expressing NahK/
 239 mut-AGX1. **b**, evaluation of tagging efficiency by feeding transfected K-562 cells DMSO, 1 μ M Ac₄GalN δ yne or 2
 240 μ M Ac₄ManNAIk. Tagging was analysed by in-gel fluorescence and quantification by densitometry as means +
 241 SD from three independent experiments. **c**, assessment of tagged glycan subtypes by treating the samples of
 242 cells fed with Ac₄GalN δ yne analysed in **b** with hydrolytic enzymes. Data are representative of one out of a total
 243 of four replicate labelling experiments performed on two different days.

244

245 MS-based validation of cell-type specific labelling in co-culture models.

246 We then validated BOCTAG as a strategy for cell-specific MS-glycoproteome analysis. We chose a co-culture
 247 model between murine 4T1 and human MCF7 breast cancer cell lines, opting to distinguish labelled
 248 glycoproteins with species-specific peptide sequences by label-free quantitative (LFQ) LC/MS-MS analysis. We
 249 transfected cells with either NahK/mut-AGX1/BH-GalNAc-T2 (termed “BOCTAG-T2”) or empty plasmid
 250 (pSBbi-Hyg, mock), co-cultured murine and human cells overnight and subsequently fed the co-cultures with
 251 either Ac₄GalN δ yne or vehicle DMSO. Chemically tagged glycoproteins in the secretome were reacted with
 252 acid-cleavable biotin-picolyl azide by CuAAC and enriched on neutravidin magnetic beads (Fig. 5a). On-bead
 253 digest yielded a peptide fraction and left glycopeptides bound to beads to be separately eluted with formic
 254 acid^{24,36,37}. Peptide samples were assessed by LFQ MS-proteomics in two independent experiments, choosing a
 255 8-fold enrichment and a p-value of 0.1 as cut-offs. We observed species-specific protein enrichment: BOCTAG-
 256 T2-expressing 4T1 cells led to 132 selectively enriched murine peptides while BOCTAG-T2-expressing MCF7
 257 cells allowed detection of 24 selectively enriched human peptides when co-cultured with mock-transfected cells

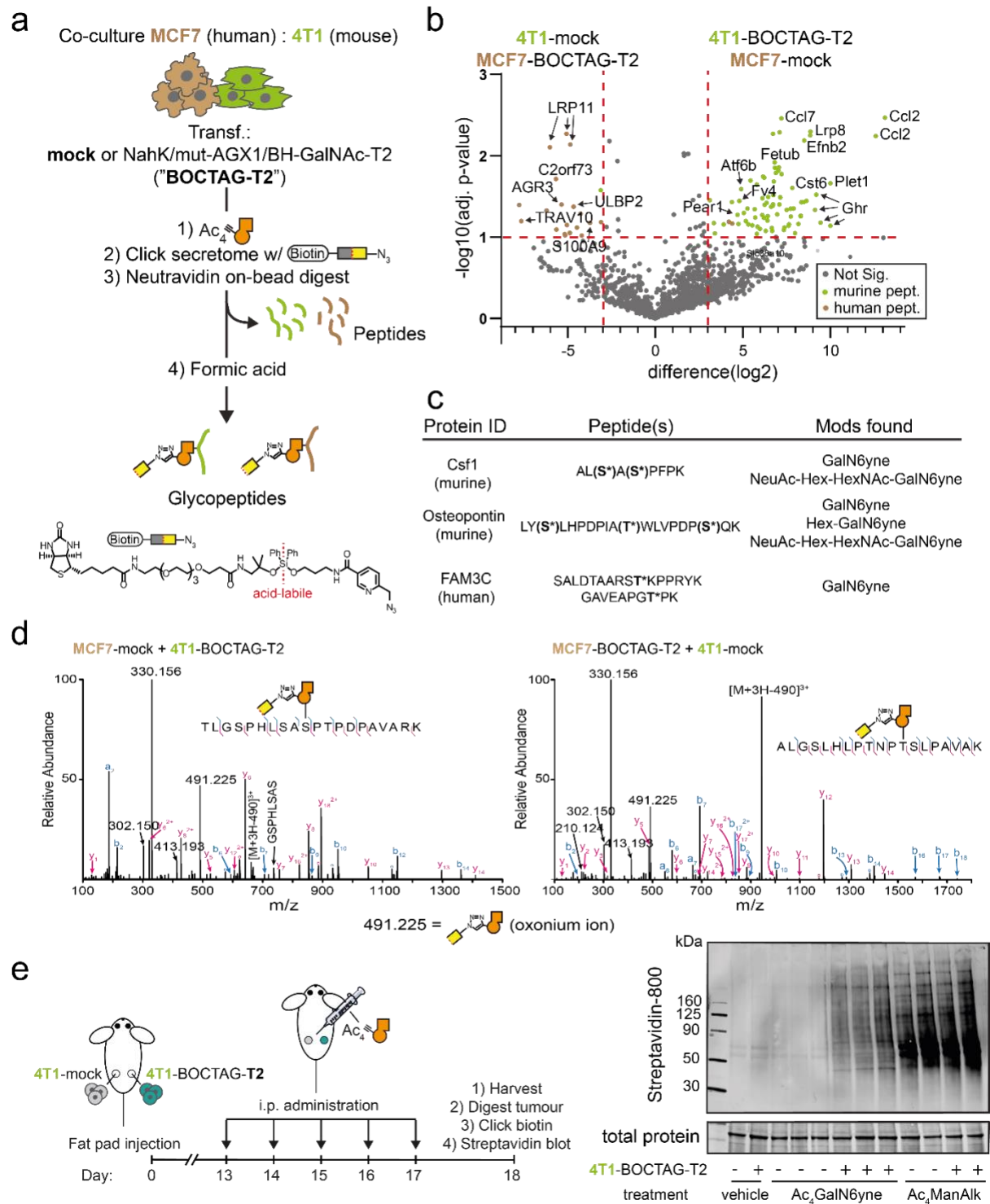
258 of the respective other species (Fig. 5b, Supplementary Table2). Only two human peptides and one murine
259 peptide were found in the enriched datasets from the corresponding other species.
260 BOCTAG-T2 allows for cell-specific glycosylation site identification. Using a tandem MS technique consisting
261 of higher energy collision dissociation (HCD)-triggered electron transfer dissociation (ETD), we identified 37
262 specific glycosylation sites on 57 murine glycopeptides from 4T1 cells and 9 specific glycosylation sites on 12
263 human glycopeptides from MCF7 cells in secretome samples (Supplementary Table2). Our data indicated
264 glycosylation of homologous glycopeptides from murine and human origins in pro-X carboxypeptidase in
265 secretome (Fig. 5d, fig. S9c). We also performed an MS-glycoproteomics experiment in lysate from the
266 4T1/MCF7 co-culture expressing BOCTAG-T2 or empty plasmid. We annotated a total of 4 specific
267 glycosylation sites on 11 murine glycopeptides from 4T1 samples and 2 specific glycosylation sites on 8 human
268 glycopeptides from MCF7 cells (Supplementary Table 3). Particularly, we identified a homologous
269 glycopeptide from both human and murine glucosidase 2 (Fig. S9b). The presence of the chemical tag facilitated
270 manual annotation of mass spectra in all cases due to the specific mass shift associated with the chemical
271 modification, in line with our own previous results.³⁸

272

273 **Bioorthogonal cell-specific tagging of glycoproteins in vivo.**

274 We next investigated the applicability of our BOCTAG strategy in an *in vivo* tumour model. Tumours were grown
275 in the fat pads of NOD-SCID IL2R^{gnull} (NSG) mice, consisting of 4T1 cells expressing GFP and either
276 BOCTAG-T2 (one fat pad) or no additional transgene (empty plasmid, another fat pad). These mice were
277 intraperitoneally injected with Ac₄GalN₆yne, vehicle or Ac₄ManNAIk once daily for five consecutive days (Fig.
278 5e). At the end of the treatment, the tumours were harvested, homogenized, treated with biotin-picolyl azide under
279 CuAAC conditions and the labelling analysed by streptavidin blot. A strong fluorescent signal was observed in
280 the BOCTAG-T2 tumours treated with Ac₄GalN₆yne (Fig 5e). In contrast, tumours transfected with empty
281 plasmid showed minimal labelling signal with either vehicle or Ac₄GalN₆yne treatment. All samples treated with
282 Ac₄ManNAIk irrespective of the presence of NahK/mut-AGX1/BH-T2 displayed strong fluorescent signal. These
283 data demonstrated that glycoproteins are selectively tagged when NahK/mut-AGX1/BH-T2 are expressed in the
284 tumour. We also performed intratumoral injections of either Ac₄GalN₆yne or DMSO and observed the same
285 BOCTAG-T2-dependent labelling (Fig. S10a).

286 To evaluate the protein expression levels of NahK/mut-AGX1/BH-T2 *ex vivo*, part of the tumours were digested,
287 plated and cells cultured. Protein expression of NahK/mut-AGX1/BH-T2 was assessed by Western blot and found
288 to be comparable to expression levels before *in vivo* injection (Fig. S10b). Cells also generally retained the ability
289 to incorporate Ac₄GalN₆yne-dependent chemical glycoproteome tagging (Fig. S10b).



290

291 **Fig. 5: BOCTAG labels glycoproteins in a cell-specific manner in co-culture and *in vivo*.** **a**, cell-selective
 292 enrichment and MS-glycoproteome analysis of murine-human co-culture systems. MCF7 and 4T1 cells
 293 transfected as indicated were co-cultured overnight and treated with DMSO or 10 μM Ac₄GalN6yne for 24h.
 294 Secretome was subjected to CuAAC with acid-cleavable biotin-picolyl azide and enriched on neutravidin beads.
 295 On-bead digest yielded peptide fractions while acid treatment of beads yielded glycopeptide fractions. **b**, MS
 296 analysis of peptide fractions from **a** by choosing 8-fold enrichment and a p-value of 0.1 as cut-offs. Species-
 297 specific peptides are indicated. Data are from two independent experiments. **c**, examples of enriched

298 glycopeptides and glycoforms. Asterisk annotates glycosylation sites; parentheses indicate potential
299 glycosylation sites that could not be confidently assigned. **d**, HCD spectra of homologous glycopeptides from
300 murine (left) and human (right) origins. Peptide sequences were confirmed by ETD (Fig S9c). **e**, *in vivo*
301 glycoproteome tagging by BOCTAG-T2. Tumours were grown in fat pads of mice as described. BOCTAG-T2
302 and mock tumours were grown in the same mouse treated systemically by intraperitoneal (i.p. administration)
303 for five days with 300 mg/kg Ac₄GalN6yne, Ac₄ManNAc or the corresponding volume of vehicle. Tumours
304 were harvested, lysed, subjected to CuAAC with biotin-picolyl azide and analysed by streptavidin blot. Hex =
305 Hexose, e.g. galactose; NeuAc = *N*-acetylneuraminic acid; HexNAc = *N*-acetylhexosamine, e.g. GlcNAc. mock:
306 pSBbi-Hyg.

307

308 DISCUSSION

309 We developed BOCTAG to address two major shortcomings in prominent research fields such as
310 cancer biology. First, there is still an unmet need for characterising proteins produced by a particular
311 cell type. Glycans are a means to an end in this respect, and the large signal-to-noise ratio in our
312 fluorescent labelling experiments indicates that BOCTAG allows for efficient protein tagging. The
313 approach is complementary to other techniques, including the use of unnatural amino acids and
314 proximity biotinylation.^{39,40} Second, directly incorporating glycans in the analysis will give insight
315 into cell-type-specific glycosylation sites and glycan structures to add another dimension to proteome
316 profiling. The presence of a modification that can be observed by MS and is a direct corollary of
317 using chemical tools allows for further validation of enriched glycoproteins, facilitating
318 glycoproteome analysis even in complex co-culture or *in vivo* settings. An artificial biosynthetic
319 pathway was essential to ensure minimal background labelling while being able to supply the tagged
320 sugar as an easy-to-synthesise MOE reagent. To this end, the use of the kinase NahK allows for use of
321 a per-acetylated bioorthogonal sugar that is fundamental to *in vivo* use and in marked difference to
322 highly unstable caged sugar-1-phosphates used previously.^{19,27} To enable BOCTAG, cells require
323 transfection with at least two transgenes. However, the design of a multicistronic, transposase-
324 responsive plasmid ensures that transfection efforts are straightforward.^{41,42} BOCTAG allowed us to
325 selectively tag tumour glycoproteomes *in vivo*, highlighting the robustness of the approach. MOE
326 reagents have been chemically caged to be released by enzymes overexpressed in cancer⁴³⁻⁴⁵. While
327 independent of transfection, such targeting can be accompanied by substantial background labelling in
328 non-cancerous tissue. BOCTAG allows for programmable glycoprotein tagging with remarkable
329 signal-to-noise ratio, and an enabling technology that will transform our understanding of tumour-host
330 interactions particularly in the context of protein glycosylation.

331

332

333 **Data availability**

334 Mass spectrometry raw sequencing data will be made available in a public repository.

335

336 **ACKNOWLEDGEMENTS**

337 We thank Mahmoud-Reza Rafiee for help with data analysis, Acely Garza-Garcia, Holly Douglas and

338 Christelle Soudy for help with chromatography, and Kayvon Pedram for providing StcE. We thank

339 Junwon Choi for UDP-sugar standards for chromatography. We thank Phil Walker for advice on

340 vector choice, and Rocco D'Antuono of the Crick Advanced Light Microscopy STP for support and

341 assistance in this work. We thank Phil East of the Bioinformatics and Biostatistics Science

342 Technology Platform for help with data analysis. We are grateful for support by the Francis Crick

343 Institute Cell Services and Peptide Chemistry Science Technology Platforms. This work was

344 supported by the Francis Crick Institute (A. C., B. C., T. R., V. B., A. M., G. B.-T., H. F., Z. L., O. Y.

345 T., C. R., P. S.-B., S. K., I. M., B. S.) which receives its core funding from Cancer Research UK

346 (FC001749, FC001045), the UK Medical Research Council (FC001749, FC001045) and Wellcome

347 Trust (FC001749, FC001045). This work was supported by the ERC (788231 to S. L. F.), the

348 Wellcome Trust (218304/Z/19/Z to A. M. and B. S.), the EPSRC (EP/S013741/1 to T. K. and M. A.

349 F., and EP/S005226/1 to S. L. F.), the BBSRC (BB/T01279X/1 to Z. L. and B. S., BB/M027791/1

350 and BB/M028836/1 to S. L. F., and BB/M02847X/1 to T. K. and M. A. F.) and the NIH (R01

351 CA200423 to C.R.B.). B.C. was supported by a Crick-HEI studentship funded by the Department of

352 Chemistry at Imperial College London and the Francis Crick Institute. For the purpose of Open

353 Access, the author has applied a CC BY public copyright licence to any Author Accepted Manuscript

354 version arising from this submission.

355 **REFERENCES**

356 1. Ombrato, L. *et al.* Metastatic-niche labelling reveals parenchymal cells with stem features.

357 *Nature* **572**, 603–608 (2019).

358 2. del Pozo Martin, Y. *et al.* Mesenchymal Cancer Cell-Stroma Crosstalk Promotes Niche

359 Activation, Epithelial Reversion, and Metastatic Colonization. *Cell Rep.* **13**, 2456–2469

- 360 (2015).
- 361 3. Yamaguchi, H. & Sakai, R. Direct interaction between carcinoma cells and cancer associated
362 fibroblasts for the regulation of cancer invasion. *Cancers (Basel)*. **7**, 2054–2062 (2015).
- 363 4. Nayak, R. & Hasija, Y. A hitchhiker’s guide to single-cell transcriptomics and data analysis
364 pipelines. *Genomics* **113**, 606–619 (2021).
- 365 5. Schoof, E. M. *et al.* Quantitative single-cell proteomics as a tool to characterize cellular
366 hierarchies. *Nat. Commun.* **12**, (2021).
- 367 6. Varki, A. & Gagneux, P. Biological Functions of Glycans. in *Essentials of Glycobiology, 3rd*
368 *edition* (2017).
- 369 7. Clausen, H., Schjoldager, K. T., Narimatsu, Y. & Joshi, H. J. Global view of human protein
370 glycosylation pathways and functions. doi:10.1038/s41580-020-00294-x.
- 371 8. Kailemia, M. J., Park, D. & Lebrilla, C. B. Glycans and glycoproteins as specific biomarkers
372 for cancer. *Anal. Bioanal. Chem.* **409**, 395–410 (2017).
- 373 9. Scott, E. & Munkley, J. Glycans as biomarkers in prostate cancer. *Int. J. Mol. Sci.* **20**, (2019).
- 374 10. Krasny, L. & Huang, P. H. Data-independent acquisition mass spectrometry (DIA-MS) for
375 proteomic applications in oncology. doi:10.1039/d0mo00072h.
- 376 11. Gauthier, N. P. *et al.* Cell-selective labeling using amino acid precursors for proteomic studies
377 of multicellular environments. *Nat. Methods* **10**, 768–773 (2013).
- 378 12. Sletten, E. M. & Bertozzi, C. R. Bioorthogonal chemistry: Fishing for selectivity in a sea of
379 functionality. *Angew. Chemie - Int. Ed.* **48**, 6974–6998 (2009).
- 380 13. Parker, C. G. & Pratt, M. R. Click Chemistry in Proteomic Investigations. *Cell* vol. 180 605–
381 632 (2020).
- 382 14. Hang, H. C., Yu, C., Kato, D. L. & Bertozzi, C. R. A metabolic labeling approach toward
383 proteomic analysis of mucin-type O-linked glycosylation. *Proc. Natl. Acad. Sci. U. S. A.* **100**,
384 14846–14851 (2003).
- 385 15. Besanceney-Webler, C. *et al.* Increasing the efficacy of bioorthogonal click reactions for
386 bioconjugation: A comparative study. *Angew. Chemie - Int. Ed.* **50**, 8051–8056 (2011).
- 387 16. Zaro, B. W., Yang, Y., Hang, H. C. & Pratt, M. R. Chemical reporters for fluorescent detection
388 and identification of O-GlcNAc-modified proteins reveal glycosylation of the ubiquitin ligase
389 NEDD4-1. **108**, 1–6 (2011).

- 390 17. Boyce, M. *et al.* Metabolic cross-talk allows labeling of O-linked β -N- acetylglucosamine-
391 modified proteins via the N-acetylgalactosamine salvage pathway. *Proc. Natl. Acad. Sci. U. S.*
392 *A.* **108**, 3141–3146 (2011).
- 393 18. Cioce, A. *et al.* Optimization of Metabolic Oligosaccharide Engineering with Ac4GalNAk
394 and Ac4GlcNAk by an Engineered Pyrophosphorylase. *ACS Chem. Biol.* (2021)
395 doi:10.1021/acscchembio.1c00034.
- 396 19. Debets, M. F. *et al.* Metabolic precision labeling enables selective probing of O-linked N -
397 acetylgalactosamine glycosylation . *Proc. Natl. Acad. Sci.* **117**, 25293–25301 (2020).
- 398 20. Pratt, M. R. *et al.* Deconvoluting the functions of polypeptide N- α -
399 acetylgalactosaminyltransferase family members by glycopeptide substrate profiling. *Chem.*
400 *Biol.* **11**, 1009–1016 (2004).
- 401 21. Broussard, A. *et al.* Human UDP-galactose 4'-epimerase (GALE) is required for cell-surface
402 glycome structure and function. *J. Biol. Chem.* **295**, 1225–1239 (2020).
- 403 22. Stanley, P. Pharmaceutical Chinese hamster ovary mutants for glycosylation engineering of
404 biopharmaceuticals. **2**, 359–361 (2014).
- 405 23. Choi, J. *et al.* Engineering Orthogonal Polypeptide GalNAc-Transferase and UDP-Sugar Pairs.
406 *J. Am. Chem. Soc.* **141**, 13442–13453 (2019).
- 407 24. Schumann, B. *et al.* Bump-and-Hole Engineering Identifies Specific Substrates of
408 Glycosyltransferases in Living Cells. *Mol. Cell* **78**, 824-834.e15 (2020).
- 409 25. Pouilly, S., Bourgeaux, V., Piller, F. & Piller, V. Evaluation of analogues of GalNAc as
410 substrates for enzymes of the Mammalian GalNAc salvage pathway. *ACS Chem. Biol.* **7**, 753–
411 760 (2012).
- 412 26. Bourgeaux, V., Piller, F. & Piller, V. Two-step enzymatic synthesis of UDP-N-
413 acetylgalactosamine. *Bioorganic Med. Chem. Lett.* **15**, 5459–5462 (2005).
- 414 27. Schumann, B. *et al.* Bump-and-Hole Engineering Identifies Specific Substrates of
415 Glycosyltransferases in Living Cells. *Mol. Cell* **78**, 824-834.e15 (2020).
- 416 28. Lewis, Y. E. *et al.* O-GlcNAcylation of α -Synuclein at Serine 87 Reduces Aggregation
417 without Affecting Membrane Binding. *ACS Chem. Biol.* **12**, 1020–1027 (2017).
- 418 29. Keenan, T. *et al.* Profiling Substrate Promiscuity of Wild-Type Sugar Kinases for Multi-
419 fluorinated Monosaccharides. *Cell Chem. Biol.* **27**, 1199-1206.e5 (2020).
- 420 30. Yu, S. *et al.* Metabolic labeling enables selective photocrosslinking of O-GlcNAc-modified

- 421 proteins to their binding partners. **109**, 1–6 (2012).
- 422 31. York, W. S. *et al.* GlyGen: Computational and Informatics Resources for Glycoscience.
423 *Glycobiology* **30**, 72–73 (2020).
- 424 32. Steentoft, C. *et al.* Precision mapping of the human O-GalNAc glycoproteome through
425 SimpleCell technology. *EMBO J.* **32**, 1478–1488 (2013).
- 426 33. Joshi, H. J. *et al.* GlycoDomainViewer: a bioinformatics tool for contextual exploration of
427 glycoproteomes. *Glycobiology* **28**, 131–136 (2018).
- 428 34. Cioce, A., Malaker, S. A. & Schumann, B. Generating orthogonal glycosyltransferase and
429 nucleotide sugar pairs as next-generation glycobiology tools. *Curr. Opin. Chem. Biol.* **60**, 66–
430 78 (2021).
- 431 35. Malaker, S. A. *et al.* The mucin-selective protease StcE enables molecular and functional
432 analysis of human cancer-associated mucins. *Proc. Natl. Acad. Sci. U. S. A.* **116**, 7278–7287
433 (2019).
- 434 36. Woo, C. M., Iavarone, A. T., Spiciarich, D. R., Palaniappan, K. K. & Bertozzi, C. R. Isotope-
435 targeted glycoproteomics (IsoTaG): a mass-independent platform for intact N- and O-
436 glycopeptide discovery and analysis. **12**, 561–567 (2015).
- 437 37. Miyamoto, D. K., Flaxman, H. A., Wu, H. Y., Gao, J. & Woo, C. M. Discovery of a Celecoxib
438 Binding Site on Prostaglandin e Synthase (PTGES) with a Cleavable Chelation-Assisted
439 Biotin Probe. *ACS Chem. Biol.* **14**, 2527–2532 (2019).
- 440 38. Calle, B. *et al.* Benefits of Chemical Sugar Modifications Introduced by Click Chemistry for
441 Glycoproteomic Analyses. *J. Am. Soc. Mass Spectrom.* **32**, 2366–2375 (2021).
- 442 39. Wei, W. *et al.* Cell type-selective secretome profiling in vivo. *Nat. Chem. Biol.*
443 doi:10.1038/s41589-020-00698-y.
- 444 40. Alvarez-Castelao, B. *et al.* Cell-type-specific metabolic labeling of nascent proteomes in vivo.
445 *Nat. Biotechnol.* **35**, 1196–1201 (2017).
- 446 41. Mátés, L. *et al.* Molecular evolution of a novel hyperactive Sleeping Beauty transposase
447 enables robust stable gene transfer in vertebrates. *Nat. Genet.* **41**, 753–761 (2009).
- 448 42. Kowarz, E., Löscher, D. & Marschalek, R. Optimized Sleeping Beauty transposons rapidly
449 generate stable transgenic cell lines. *Biotechnol. J.* **10**, 647–653 (2015).
- 450 43. Shim, M. K. *et al.* Cathepsin B-Specific Metabolic Precursor for In Vivo Tumor-Specific
451 Fluorescence Imaging. *Angew. Chemie - Int. Ed.* **55**, 14698–14703 (2016).

- 452 44. Shim, M. K. *et al.* Caspase-3/-7-Specific Metabolic Precursor for Bioorthogonal Tracking of
453 Tumor Apoptosis. *Sci. Rep.* **7**, 1–15 (2017).
- 454 45. Wang, H. *et al.* Selective in vivo metabolic cell-labeling-mediated cancer targeting. *Nat.*
455 *Chem. Biol.* **13**, 415–424 (2017).
- 456